NANO LETTERS

Letter

pubs.acs.org/NanoLett

Vapor Trapping Growth of Single-Crystalline Graphene Flowers: Synthesis, Morphology, and Electronic Properties

Yi Zhang,[†,‡,∥] Luyao Zhang,[†,§,∥] Pyojae Kim,[†] Mingyuan Ge,[§] Zhen Li,[†] and Chongwu Zhou*[,†,‡,§]

[†]Department of Electrical Engineering, [‡]Department of Chemistry, and [§]Department of Chemical Engineering and Materials Science, University of Southern California, Los Angeles, California 90089, United States

Supporting Information

ABSTRACT: We report a vapor trapping method for the growth of large-grain, single-crystalline graphene flowers with grain size up to 100 μm. Controlled growth of graphene flowers with four lobes and six lobes has been achieved by varying the growth pressure and the methane to hydrogen ratio. Surprisingly, electron backscatter diffraction study revealed that the graphene morphology had little correlation with the crystalline orientation of underlying copper substrate. Field effect transistors were fabricated based on graphene flowers and the fitted device mobility could achieve ~4200 $cm^2 V^{-1} s^{-1}$ on Si/SiO_2 and ~20 000 $cm^2 V^{-1} s^{-1}$ on hexagonal boron nitride (h-BN). Our vapor trapping method provides a viable way for large-grain single-crystalline graphene synthesis for potential high-performance graphene-based electronics.

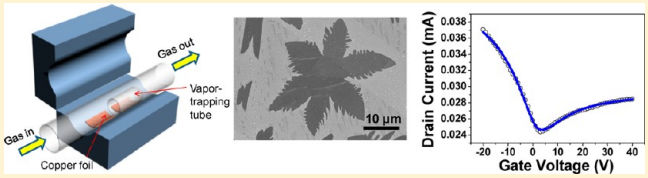

KEYWORDS: *Vapor trapping, graphene growth, large-grain graphene, morphology, graphene transistors*

Graphene is a two-dimensional, honeycomb lattice arrangement with unique physical properties.[1−4] To overcome the disadvantage of small-scale production of graphene using mechanical exfoliation of highly orientated polymeric graphite (HOPG), chemical vapor deposition (CVD) of large-area single-layer graphene on metal films has been explored from various aspects.[5−11] Despite the significant progress, CVD graphene is usually a polycrystalline film made of small grains.[12] As the grain boundaries have been found to impede both transport[11,13,14] and mechanical properties,[15] it is therefore very important to be able to synthesize large-grain, single-crystalline graphene for various applications. The pioneering work of Li et al.[10] demonstrated the CVD growth of large graphene single crystals up to 0.5 mm in size, using a copper enclosure. Such large graphene single crystals can be very important and may find applications for various electronic devices, however, the process depends on how the copper enclosure is manually made, and the copper enclosure does not allow probing the gas environment inside. Because of the utmost importance, alternative means to produce large-grain single-crystalline graphene can be very beneficial for applications and the growth mechanism study.

In this work, we report a vapor trapping method to grow large-grain, single-crystalline graphene with controlled grain morphology. The grain size of six-lobe-flower-shape grains can achieve 100 μm with high quality single-layer graphene as lobes and bilayer graphene as centers. Selected area electron diffraction (SAED) has been applied to confirm the single-crystalline nature of the graphene flowers, and systematic study of the graphene morphology versus growth parameters (total pressure and methane-to-hydrogen ratio) has been performed. We found that the graphene morphology can be well controlled by tuning the total pressure of the CVD system, and the methane-to-hydrogen ratio. In addition, electron backscatter diffraction (EBSD) study indicates that the graphene morphology has little correlation with the crystal orientation of the underlying copper substrate. Field-effect transistors (FETs) have been fabricated based on the large-grain graphene flowers, and the fitted device mobility could achieve ~4200 $cm^2 V^{-1} s^{-1}$ on Si/SiO_2 and ~20 000 $cm^2 V^{-1} s^{-1}$ on hexagonal boron nitride (h-BN).

Graphene synthesis was done using a vapor trapping chemical vapor deposition method as illustrated in Figure 1a. Cu foil was rolled up and put into a half inch small quartz tube, which is open only at one end. The half inch quartz tube was then placed inside a two inch quartz tube of the CVD chamber. Gases flown into the small quartz tube would be trapped inside, and therefore we believe that the small quartz tube would result in gas composition and gas flow rate different from outside the tube, thus leading to interesting growth results of graphene. Another piece of Cu foil was sometimes placed outside the small vapor trapping tube for comparison. Seven standard cubic centimeters per minute H_2 was introduced to the CVD chamber at 40 mTorr, and the temperature was brought up to 1000 °C in 40 min. The Cu foils were annealed at 1000 °C for 20 min. One standard cubic centimeters per minute CH_4 and 12.5 sccm H_2 were then introduced into the CVD chamber for graphene growth. The pressure was kept at 200 mTorr for 30 min during the growth. The CVD chamber was cooled down to room temperature with the flow of 1 sccm CH_4 and 12.5 sccm

Received: January 4, 2012
Revised: April 2, 2012
Published: April 26, 2012

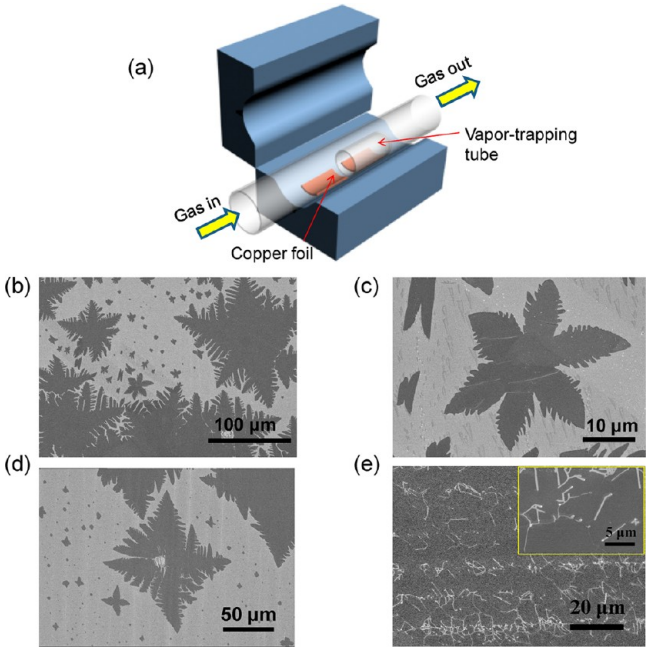

Figure 1. (a) Schematic diagram of a vapor trapping CVD method for graphene growth. (b) Low and (c) high-magnification SEM images of a six-lobe graphene flower grown on Cu foil inside the vapor trapping tube. (d) SEM image of a four-lobe graphene flower grown on Cu foil inside the vapor trapping tube. (e) Graphene grown on Cu foil outside the vapor-trapping tube.

H_2 continuing. Figure 1b,c shows SEM images of six-lobe graphene flowers grown on the bottom side of Cu foil placed inside the vapor trapping tube. The size of graphene flowers is up to 100 μm (Figure 1b). By varying the growth parameters, we also observed four-lobe graphene flowers grown on Cu foil as shown in Figure 1d. Interestingly, the graphene grown on the Cu foil placed outside the small vapor trapping tube did not show any "flower" shape, but continuous graphene film with slight etching[16] was found instead (Figure 1e). The pronounced difference between graphene grown on Cu foil inside and outside the vapor-trapping tube indicates that the vapor trapping tube does change the local environment inside the tube, especially in reducing the carbon supply and creating a quasi-static reactant gas distribution that results in large flower-shaped graphene grains. We also observed graphene flowers grown on copper foil without the vapor trapping tube by using reduced methane flow rate (Supporting Information Figure S1); however, the shape of flowers was not as uniform as the ones using the vapor trapping tube. Our vapor trapping approach has little variation from run to run, and the open end of the vapor trapping tube may enable probing of gas species inside using techniques such as mass spectrometer.

The graphene flowers were successfully transferred onto Si/SiO_2 substrates for further investigation using the reported transfer technique.[5] Scanning electron microscopy (SEM) image and optical microscope image of a six-lobe graphene flower are shown in Figure 2a,b. The color contrast of the graphene flower is very uniform in both SEM and the optical image, except that the central part takes a hexagonal shape and is darker than the lobes. Raman spectra were taken from different locations on the transferred graphene sample. The Raman spectrum in black in Figure 2c was taken from the area outside the graphene flower (marked by letter A in Figure 2b), which did not show any G or 2D peak of graphene as expected. In contrast, the Raman spectrum in red in Figure 2c was taken from the area of graphene lobes (marked by letter B in Figure 2b). It presents typical features of single-layer graphene: the I_{2D}/I_G intensity ratio is ~0.5, and the full width at half-maximum (fwhm) of 2D band is ~33 cm^{-1}. The Raman spectrum in blue in Figure 2c was collected from the center of the graphene flower (marked by letter C in Figure 2b). The I_{2D}/I_G intensity ratio is ~1 and the fwhm of 2D band ~53 cm^{-1}, which represents bilayer graphene.[17] To further investigate large surface area of the graphene flower, Raman maps of I_G, I_{2D}, and I_{2D}/I_G intensity ratio were collected and shown in Figure 2d, e, and f, respectively. The maps show very uniform G and 2D band for the graphene flower with only a

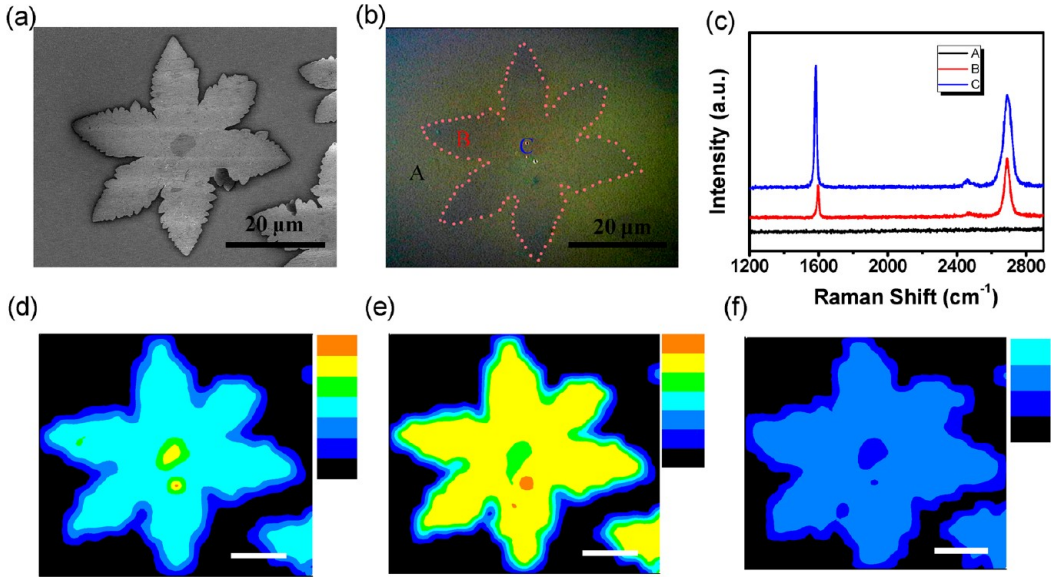

Figure 2. (a) A SEM image and (b) an optical microscope image of a six-lobe graphene flower transferred on a Si/SiO_2 substrate. (c) Raman spectra taken from location A, B, and C marked in Figure 2b. (d–f) Raman map of I_G, I_{2D}, and I_{2D}/I_G intensity ratio. Scale bar for (d–f) is 10 μm. The color scale bar from bottom to top is 300, 500, 900, 1300, 1700, 2000 (d); 100, 600, 1200, 1800, 2400, 3200 (e); 1, 2, 3 (f).

dx.doi.org/10.1021/nl300039a | Nano Lett. 2012, 12, 2810–2816

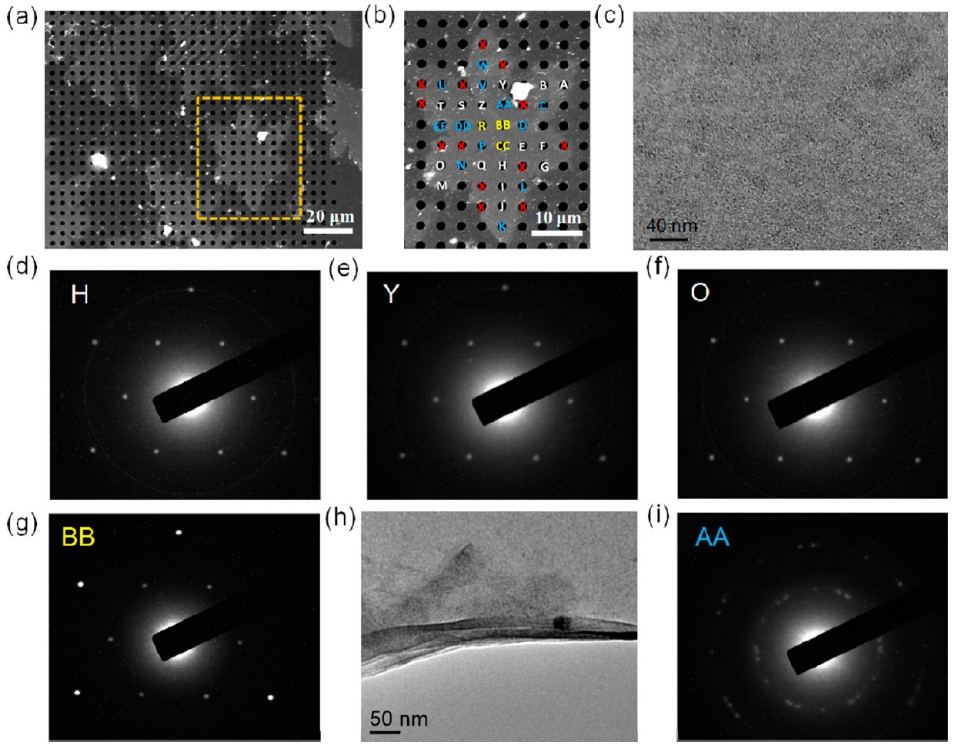

Figure 3. (a) SEM image of graphene flowers transferred on a perforated silicon nitride TEM grid. (b) Zoomed-in SEM image of the graphene flower marked using yellow dashed square in panel a. Each opening within the graphene flower was marked by a letter (white, single-layer graphene; yellow, A−B stacking bilayer graphene; blue, torn and folded graphene) or a red cross (no graphene covered). (c) A bright-field TEM image of graphene suspended on silicon nitride TEM grid. (d−f) Diffraction patterns taken from opening H, Y, and O, respectively. (g) Diffraction pattern taken from opening BB. (h) A bright-field TEM image of torn and folded graphene taken from opening AA. (i) Diffraction pattern taken from opening AA.

little PMMA residue on the lower lobe. Therefore, Raman spectroscopy shows that the graphene flower is mainly single-layer graphene with a small bilayer region in the center, which is believed to be the nucleation site.

The grain size of graphene is of great importance in device application since grain boundaries may affect the transport properties of graphene FETs, and decrease the device mobility. Previously low energy electron microscopy (LEEM) was used to investigate graphene grain size,[10] but access to LEEM is usually not widely available. Here we report the use of SAED as a reliable method to study the crystalline structure and grain size of graphene, which can be performed with readily available transmission electron microscopy (TEM). As-grown graphene flowers were transferred onto a perforated silicon nitride TEM grid. SEM image of graphene on TEM grid in Figure 3a shows that graphene retains its flower shape after transfer. Figure 3b is a zoomed-in SEM image of the graphene flower highlighted by yellow dashed line in Figure 3a. In order to measure the grain size of graphene, we did SAED on graphene at every opening within the graphene flower, and compared the orientation of the diffraction patterns. As shown in Figure 3b, three different kinds of diffraction patterns were marked by white letters, yellow letters, and blue letters, respectively. The openings which were not covered by graphene membrane were marked by red crosses. Figure 3c shows a bright field TEM image of graphene membrane at a TEM grid opening covered by graphene membrane. The graphene membrane is clean, uniform, and smooth within the opening. We observe that the openings marked with white letters all show one set of symmetric 6-fold electron diffraction pattern that orientates to the same direction. Figure 3d−f shows images of three representative diffraction patterns from opening H, Y, and O. One can see that the openings with white letters cover all six lobes of the graphene flower, indicating that the graphene flower is a single-crystalline grain.

Figure 3g shows the diffraction pattern taken from the opening BB located at the center of the graphene flower, also displaying one set of symmetric 6-fold diffraction spots. The outer set of diffraction spots are from equivalent planes {1−210}, showing higher (approximately twice) intensity than the inner set from {1−100}. This is a key feature for A−B stacking bilayer graphene.[18] This observation is also in accordance with the Raman spectra (Figure 2c) showing that the center of graphene flower consists of bilayer graphene. We also observed that the graphene membrane was torn or folded at some of the openings of the TEM grid. This might be due to the surface tension caused by the transfer process. Figure 3h shows a bright-field TEM image taken from opening AA, which is covered by torn and folded graphene film. The folded graphene membrane becomes multiple-layered, and hence the diffraction patterns taken from folded graphene membrane show multiple sets of diffraction spots in Figure 3i. We marked all the openings with torn and folded graphene membrane with blue letters, and their diffraction patterns are all similar to the one shown in Figure 3i. Once we exclude torn and folded graphene due to the transfer, we can conclude that SAED on each opening covered by the graphene flower confirms that the graphene flower is a single-crystalline graphene grain, and the center of the graphene flower is A−B stacking bilayer graphene.

dx.doi.org/10.1021/nl300039a | *Nano Lett.* 2012, 12, 2810−2816

During our synthesis process, it was observed that the morphology of large graphene grains changed when the parameters changed in the CVD system. Among various growth parameters, the total pressure of the CVD system and methane-to-hydrogen ratio were found to be two important parameters that were closely related to the morphology of graphene grains. To investigate the correlation between the grain morphology and the total pressure and methane-to-hydrogen ratio, we varied the total pressure at a fixed methane to hydrogen ratio (1:12.5), and also varied methane-to-hydrogen ratio at a fixed total pressure (150 mT) to conduct a series of growth process. Figure 4 shows the growth results

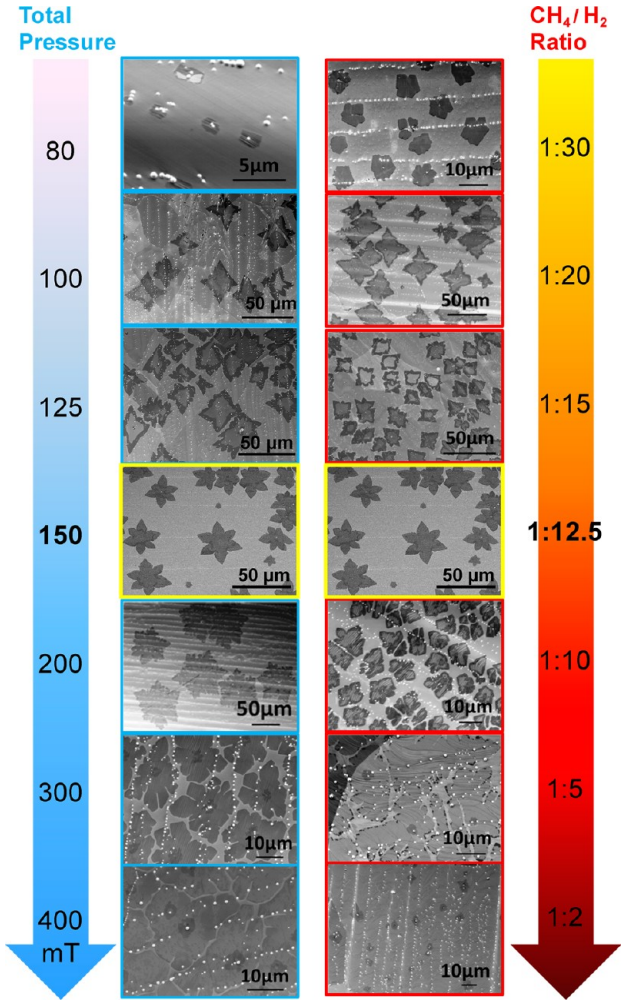

Figure 4. SEM images of graphene grown using various recipe. The central images with yellow frame in both left and right column are the same. And the graphene was grown at 150 mTorr using 1:12.5 CH_4/H_2 ratio. The left set of SEM images with blue frame are graphene grown at 1:12.5 CH_4/H_2 ratio with the total pressure varied from 80 mTorr to 400 mTorr. The right set of SEM images with red frame are graphene grown at 150 mTorr with CH_4/H_2 concentration ratio varied from 1:30 to 1:2.

using various conditions when a reaction time of 30 min was used. With methane-to-hydrogen ratio of 1:12.5, we carried out graphene CVD using the vapor trapping method at total pressure of 80, 100, 125, 150, 200, 300, and 400 mTorr. Corresponding SEM images are shown in the left column in Figure 4. We observed that the graphene grains changed from irregular small flakes (80 mTorr) to mostly four-lobe grains (100 mTorr), and then changed to irregular patterns in between four-lobe and six-lobe flowers (125 mTorr), then to mostly six-lobe flowers (150 and 200 mTorr). When we further increased the total pressure to 300 mTorr, the six-lobe graphene flowers turned to irregular shape when a reaction time of 30 min was used. The individual graphene grains tended to coalesce with each other when the total pressure was increased to 400 mTorr, leaving small gaps between irregular graphene grains. Interestingly, similar results were obtained when we kept the total pressure at 150 mTorr and gradually increased the methane to hydrogen ratio from 1:30 to 1:2. As shown in the right column of SEM images in Figure 4, graphene grains were small and close to hexagonal shape at 1:30 ratio, and then the graphene grains changed to mostly four-lobe structures when the methane-to-hydrogen ratio increased to 1:20. The grains exhibited shape between four-lobe and six-lobe flowers for CH_4/H_2 = 1:15 and exhibited mostly six-lobe flowers for CH_4/H_2 = 1:12.5. When we further increased the methane to hydrogen ratio to 1:10, the graphene grains became irregular. For CH_4/H_2 = 1:5, the graphene islands tended to connect with each other, leaving only small gaps in between. When methane-to-hydrogen ratio was brought up to 1:2, graphene grew into continuous film with multilayer patches in some locations. All the observations indicate that increasing the total pressure of the CVD system has a similar effect on the morphology of graphene grains as increasing the methane-to-hydrogen ratio. The morphology of graphene grains changed from small irregular flakes to graphene flowers with lobe structures, and eventually coalesced into a quasi continuous graphene film with the increase of total pressure or methane-to-hydrogen ratio. We believe that the graphene growth is a balance between carbon diffusion/deposition and hydrogen etching.[16] When the carbon supply is low (at low CH_4/H_2 ratio or low total pressure), the graphene nucleates and forms some initial structures, but the grains of graphene are small because of limited carbon supply and the etching effect of hydrogen. When the carbon supply increases, carbon diffuse along particular directions to grow into graphene lobes, and when the carbon supply increases further, the graphene grains grow close to each other and the original along-the-lobe carbon diffusion is perturbed. The morphology of graphene depends on both CH_4/H_2 ratio and the total pressure as the underlying mechanism includes both carbon diffusion/deposition and hydrogen etching.

In addition, we carried out graphene CVD under the pressure of 300 mTorr using different growth time with results shown in Supporting Information Figure S2. We observed lobed graphene flowers with growth time of 5 and 10 min. When growth time of 20 and 30 min were used, the graphene grains grew close to each other, and the morphology became irregular due to disturbed diffusion path of carbon by adjacent flakes.

To further study the correlation between the morphology of graphene grains and the underneath copper surface, electron backscatter diffraction (EBSD) was used to investigate the copper surface after graphene growth. Figure 5 shows EBSD images of copper surface covered by graphene flowers with different shapes. Figure 5a–c shows SEM images of graphene flowers grown at different locations on the same copper substrate (CH_4/H_2 = 1:12.5, 200 mTorr) with images taken with the sample tilted at 70° for EBSD. The graphene grains on this sample were mostly six-lobe flowers (e.g., Figure 5b), with a few four-lobe flowers in some locations (e.g., Figure 5a,c).

dx.doi.org/10.1021/nl300039a | *Nano Lett.* 2012, 12, 2810–2816

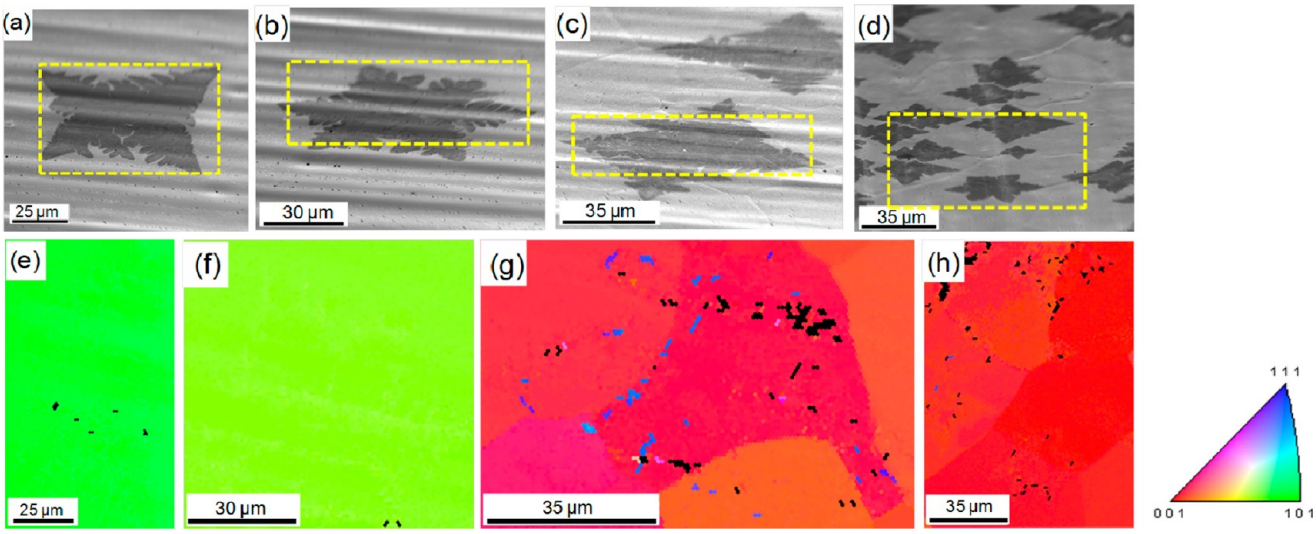

Figure 5. (a) SEM image of a four-lobe graphene flower, (b) a six-lobe graphene flower, and (c) another four-lobe graphene flower on the same graphene sample. (d) SEM image of a sample with six-lobe, and four-lobe graphene flowers, and copper grain boundaries. All SEM images (a–d) were taken with samples tilted at 70° along *Y* axis. (e–h) Corresponding EBSD orientation map image of the location highlighted by the yellow dashed square in e, f, g, and h, respectively. The color represents fcc crystalline orientation is shown on the right side.

Corresponding EBSD orientation map images for the locations highlighted by yellow dashed squares in Figure 5a–c are shown in Figure 5f–h, respectively. EBSD orientation map image in Figure 5e,f shows similar but slightly different green colors that are close to Cu(110), as indicated in the color scale bar. EBSD orientation map in Figure 5g shows orange-magenta color, indicating a crystal orientation close to Cu(100). All the above information indicates that graphene grains can grow into different morphology on the same copper substrate, and the underneath copper crystalline orientation is not closely related to the morphology of the graphene grains grown on top. Moreover, we investigated a sample with copper grain boundaries and both four- and six-lobe graphene flowers grown on the surface. Figure 5d shows a SEM image of a graphene sample grown using a different recipe (CH_4/H_2 = 1:12.5, 125 mTorr). Copper grain boundaries and both four- and six-lobe graphene flowers are shown in the SEM image. The corresponding EBSD orientation map of the highlighted location using a yellow dashed square in Figure 5h shows crystalline index close to Cu(100), with slight orientation difference between adjacent copper grains. The black points in the EBSD images correspond to locations where the instrument cannot determine the crystal orientation with high confidence. The results from EBSD indicate that for the CVD growth on polycrystalline copper foil, the morphology of graphene grains do not have much correlation with the crystalline structure of the underneath copper substrate. In fact, both four-lobe[13,19,20] and six-lobe[10,21] graphene morphology have been observed and reported by many research groups on polycrystalline copper foil[10,13,19,21] or single crystal copper.[20] Recently, Rasool et al.[20] reported that the interaction between graphene and underneath copper substrate was weak, and since the copper atoms are almost freely mobile, they may act as carbon carriers to extend the graphene grains. Therefore, we believe that the morphology of graphene grains is mostly related to the local environment close to the copper substrate and can be tuned by varying growth parameters (pressure, methane-to-hydrogen ratio, flow rate, and so forth) but the graphene morphology does not have much correlation with the beneath copper substrate.

To evaluate the quality of the large-grain single-crystalline graphene flowers, we transferred the as-grown graphene grains onto a highly doped p-type silicon substrate with 300 nm thermal oxide as the gate dielectric and fabricated back-gated graphene FETs. Five nanometers Ti and fifty nanometers Pd were deposited as source and drain electrodes by e-beam evaporation. Figure 6a shows an SEM image of the graphene FET. Five electrodes were marked from A to E, and a central electrode was marked as F. Figure 6b shows a representative plot (shown in black circles) of drain current (I_{ds}) versus gate voltage (V_g) minus Dirac point voltage (V_{Dirac}) using D and F

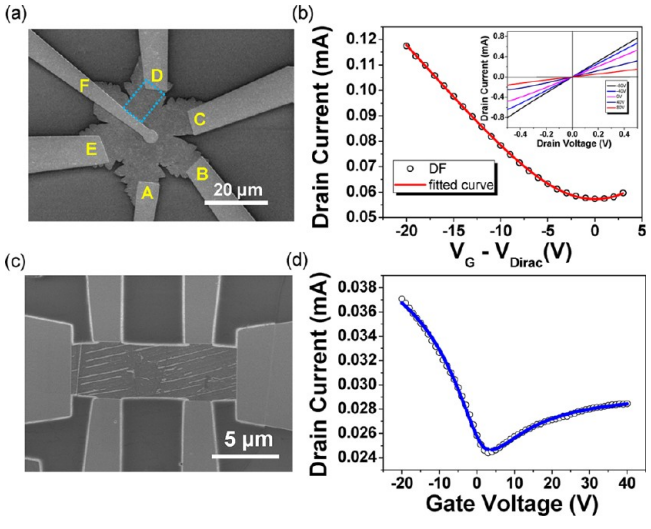

Figure 6. (a) SEM image of a six-lobe graphene FET. Electrodes are marked by different letters. The dashed blue square is the region of effective graphene channel between electrode D and F. (b) Plot of drain current (I_{ds}) versus gate voltage (V_g) minus Dirac point voltage (V_{Dirac}) using D and F as source and drain electrodes (black circles) and fitted FET mobility curve (solid red line). The drain voltage (V_{ds}) is 0.2 V. Inset is a plot of drain current (I_{ds}) versus drain voltage (V_{ds}) at various gate voltages. (c) SEM image of a hall-bar graphene/h-BN FET. (d) Plot of drain current (I_{ds}) versus gate voltage (V_g).

dx.doi.org/10.1021/nl300039a | *Nano Lett.* 2012, 12, 2810–2816

as source and drain electrodes. The drain voltage (V_{ds}) is 0.2 V. We fitted the curve to retrieve the field effect mobility μ_{FE} using the equation

$$R_{total} = \frac{1}{e\mu_{FE}\sqrt{n_0^2 + n^2}}\frac{L}{W} + R_c \quad (1)$$

where $R_{total} = V_{ds}/I_{ds}$ is the total resistance of the device including the channel resistance and contact resistance R_c, e is the electron charge, L and W are the length and width of the graphene channel, respectively, and n_0 and n are the carrier density due to residual impurities and back-gate modulation, respectively.[22] The capacitive carrier density n is related to the gate voltage via the equation

$$V_{BG} - V_{Dirac} = \frac{ne}{C_{ox}} \quad (2)$$

where the term on the right-hand side of eq 2 describe the carrier density induced by the back gate via the back-gate electrostatic capacitance C_{ox}. We did not include the quantum capacitance in graphene on the right-hand side of eq 2 since it was negligible compared to the back-gate induced carrier density in our back-gated devices. We fitted the back-gated device DF using this method, and the red curve shown in Figure 6b was the curve for fitted field effect mobility. Without a well-defined channel of the device, we estimated the device dimension by using the region of graphene grain marked by the dashed blue rectangular. The estimated L and W were 12 and 7.5 μm, and the fitted field effect mobility was ~4,200 $cm^2V^{-1}s^{-1}$. This value is comparable with the mobility of large single crystal graphene reported recently,[10] indicating the high quality of the synthesized graphene flowers. The inset of Figure 6b is a plot of drain current (I_{ds}) versus drain voltage (V_{ds}) at various gate voltages. The drain current increases linearly with the increase of drain voltage at different gate voltages, indicating the Ohmic contact between graphene and Pd electrodes. Since much higher mobility can be expected for graphene flowers transferred to h-BN as reported for CVD graphene,[23,24] we transferred large-grain graphene flowers onto exfoliated h-BN and subsequently fabricated hall-bar devices as shown in Figure 6c. Figure 6d shows a plot (shown in black circles) of drain current (I_{ds}) versus gate voltage (V_g) of one of the graphene/h-BN devices, with a channel length of 13.5 μm and width of 4.5 μm. We also fitted the curve with the same equation used in the back-gated device on Si/SiO_2 (shown in blue curve in Figure 6d). The extracted hole and electron mobility is ~10 000 $cm^2 V^{-1} s^{-1}$ and ~20 000 $cm^2 V^{-1} s^{-1}$, respectively. The previously reported mobility at room temperature of small-grain CVD graphene/h-BN was ~1200 $cm^2V^{-1} s^{-1}$ from Kim et al.[24] and from 8000 to 13 000 $cm^2 V^{-1} s^{-1}$ from Gannett et al.[23] Our large-grain graphene flower shows great potential for the application of high mobility graphene-based nanoelectronics.

In summary, we developed a vapor trapping method to grow large-grain, single-crystalline graphene with controlled grain morphology and grain size up to 100 μm. Raman spectra indicate that the graphene flowers have high quality single-layer graphene as lobes and bilayer graphene as centers. SAED confirms the single-crystalline nature of graphene flowers. Systematic study of the graphene morphology versus growth parameters and EBSD study indicate that the graphene morphology mostly relates to the local environment around the growth area and does not have much correlation with the crystalline orientation of the underneath copper substrate. FETs have been fabricated based on the large-grain graphene flowers, and high device mobility ~4200 $cm^2 V^{-1} s^{-1}$ on Si/SiO_2 and ~20 000 $cm^2 V^{-1} s^{-1}$ on h-BN have been achieved, indicating that the large-grain single-crystalline graphene is of great potential for graphene-based nanoelectronics. Further effort toward location controlled growth of single-crystalline graphene flowers of even larger grain size is currently underway.

■ ASSOCIATED CONTENT

Supporting Information

Graphene growth using reduced methane flow rate without vapor trapping tube., and time evolution of graphene growth at 300 mTorr. This material is available free of charge via the Internet at http://pubs.acs.org.

■ AUTHOR INFORMATION

Corresponding Author

*E-mail: chongwuz@usc.edu.

Author Contributions

‖These authors contributed equally to this work

Notes

The authors declare no competing financial interest.

■ ACKNOWLEDGMENTS

We acknowledge the financial support from the Focus Center Research Program (FCRP) - Center on Functional Engineered Nano Architectonics (FENA) and Office of Naval Research (ONR). We thank Professor Stephen Cronin for access to micro Raman system.

■ REFERENCES

(1) Geim, A. K.; Novoselov, K. S. The Rise of Graphene. *Nat. Mater.* **2007**, *6*, 183−191.

(2) Novoselov, K. S.; Geim, A. K.; Morozov, S. V.; Jiang, D.; Zhang, Y.; Dubonos, S. V.; Grigorieva, I. V.; Firsov, A. A. Electric Field Effect in Atomically Thin Carbon Films. *Science* **2004**, *306*, 666−669.

(3) Novoselov, K. S.; Geim, A. K.; Morozov, S. V.; Jiang, D.; Katsnelson, M. I.; Grigorieva, I. V.; Dubonos, S. V.; Firsov, A. A. Two-Dimensional Gas of Massless Dirac Fermions in Graphene. *Nature* **2005**, *438*, 197−200.

(4) Zhang, Y. B.; Tan, Y. W.; Stormer, H. L.; Kim, P. Experimental Observation of the Quantum Hall Effect and Berry's Phase in Graphene. *Nature* **2005**, *438*, 201−204.

(5) De Arco, L. G.; Zhang, Y.; Kumar, A.; Zhou, C. W. Synthesis, Transfer, and Devices of Single- and Few-Layer Graphene by Chemical Vapor Deposition. *IEEE Trans. Nanotechnol.* **2009**, *8*, 135−138.

(6) Yu, Q. K.; Lian, J.; Siriponglert, S.; Li, H.; Chen, Y. P.; Pei, S. S. Graphene Segregated on Ni Surfaces and Transferred to Insulators. *Appl. Phys. Lett.* **2008**, *93*, 113103.

(7) Kim, K. S.; Zhao, Y.; Jang, H.; Lee, S. Y.; Kim, J. M.; Kim, K. S.; Ahn, J. H.; Kim, P.; Choi, J. Y.; Hong, B. H. Large-scale Pattern Growth of Graphene Films for Stretchable Transparent Electrodes. *Nature* **2009**, *457*, 706−710.

(8) Reina, A.; Jia, X. T.; Ho, J.; Nezich, D.; Son, H. B.; Bulovic, V.; Dresselhaus, M. S.; Kong, J. Large Area, Few-Layer Graphene Films on Arbitrary Substrates by Chemical Vapor Deposition. *Nano Lett.* **2009**, *9*, 30−35.

(9) Li, X. S.; Cai, W. W.; An, J. H.; Kim, S.; Nah, J.; Yang, D. X.; Piner, R.; Velamakanni, A.; Jung, I.; Tutuc, E. Large-Area Synthesis of High-Quality and Uniform Graphene Films on Copper Foils. *Science* **2009**, *324*, 1312−1314.

(10) Li, X. S.; Magnuson, C. W.; Venugopal, A.; Tromp, R. M.; Hannon, J. B.; Vogel, E. M.; Colombo, L.; Ruoff, R. S. Large-Area Graphene Single Crystals Grown by Low-Pressure Chemical Vapor

Deposition of Methane on Copper. *J. Am. Chem. Soc.* **2011**, *133*, 2816−2819.
(11) Yu, Q. K.; Jauregui, L. A.; Wu, W.; Colby, R.; Tian, J. F.; Su, Z. H.; Cao, H. L.; Liu, Z. H.; Pandey, D.; Wei, D. G. Control and Characterization of Individual Grains and Grain Boundaries in Graphene Grown by Chemical Vapour Deposition. *Nat. Mater.* **2011**, *10*, 443−449.
(12) Huang, P. Y.; Ruiz-Vargas, C. S.; van der Zande, A. M.; Whitney, W. S.; Levendorf, M. P.; Kevek, J. W.; Garg, S.; Alden, J. S.; Hustedt, C. J.; Zhu, Y.; Park, J.; McEuen, P. L.; Muller, D. A. Grains and Grain Boundaries in Single-Layer Graphene Atomic Patchwork Quilts. *Nature* **2011**, *469*, 389.
(13) Li, X. S.; Magnuson, C. W.; Venugopal, A.; An, J. H.; Suk, J. W.; Han, B. Y.; Borysiak, M.; Cai, W. W.; Velamakanni, A.; Zhu, Y. W.; Fu, L. F.; Vogel, E. M.; Voelkl, E.; Colombo, L.; Ruoff, R. S. Graphene Films with Large Domain Size by a Two-Step Chemical Vapor Deposition Process. *Nano Lett.* **2010**, *10*, 4328−4334.
(14) Yazyev, O. V.; Louie, S. G. Electronic Transport in Polycrystalline Graphene. *Nat. Mater.* **2010**, *9*, 806−809.
(15) Shenoy, V. B.; Grantab, R.; Ruoff, R. S. Anomalous Strength Characteristics of Tilt Grain Boundaries in Graphene. *Science* **2010**, *330*, 946−948.
(16) Zhang, Y.; Li, Z.; Kim, P.; Zhang, L.; Zhou, C. W. Anisotropic Hydrogen Etching of Chemical Vapor Deposited Graphene. *ACS Nano* **2011**, *6*, 126−132.
(17) Chen, S. S.; Cai, W. W.; Piner, R.; Suk, J. W.; Wu, Y. P.; Ren, Y. J.; Kang, J. Y.; Ruoff, R. S., Synthesis and Characterization of Large-Area Graphene and Graphite Films on Commercial Cu-Ni Alloy Films. *Nano Lett.* **2011**, ASAP.
(18) Liu, Z. F.; Yan, K.; Peng, H. L.; Zhou, Y.; Li, H. Formation of Bilayer Bernal Graphene: Layer-by-Layer Epitaxy via Chemical Vapor Deposition. *Nano Lett.* **2011**, *11*, 1106−1110.
(19) Wofford, J. M.; Nie, S.; McCarty, K. F.; Bartelt, N. C.; Dubon, O. D. Graphene Islands on Cu Foils: The Interplay between Shape, Orientation, and Defects. *Nano Lett.* **2010**, *10*, 4890−4896.
(20) Rasool, H. I.; Song, E. B.; M., M.; Regan, B. C.; Wang, K. L.; Weiller, B. H.; Gimzewski, J. K. Atomic-Scale Characterization of Graphene Grown on Copper (100) Single Crystals. *J. Am. Chem. Soc.* **2011**, *133*, 12536−12543.
(21) Vlassiouk, I.; Regmi, M.; Fulvio, P.; Dai, S.; Datskos, P.; Eres, G.; Smirnov, S. Role of Hydrogen in Chemical Vapor Deposition Growth of Large Single-Crystal Graphene. *ACS Nano* **2011**, *5*, 6069−6076.
(22) Zhang, Z. Y.; Wang, Z. X.; Xu, H. L.; Wang, S.; Ding, L.; Zeng, Q. S.; Yang, L. J.; Pei, T. A.; Liang, X. L.; Gao, M.; Peng, L. M. Growth and Performance of Yttrium Oxide as an Ideal High-k Gate Dielectric for Carbon-Based Electronics. *Nano Lett.* **2010**, *10*, 2024−2030.
(23) Gannett, W.; Regan, W.; Watanabe, K.; Taniguchi, T.; Crommie, M. F.; Zettl, A. Boron Nitride Substrates for High Mobility Chemical Vapor Deposited Graphene. *Appl. Phys. Lett.* **2011**, 98.
(24) Kim, E.; Yu, T. H.; Song, E. S.; Yu, B. Chemical Vapor Deposition-Assembled Graphene Field-Effect Transistor on Hexagonal Boron Nitride. *Appl. Phys. Lett.* **2011**, 98.